

# Gene-MOE: A sparsely gated prognosis and classification framework exploiting pan-cancer genomic information

Xiangyu Meng, Xue Li, Qing Yang, Huanhuan Dai, Lian Qiao, Hongzhen Ding, Long Hao, Xun Wang

**Abstract**—Deep learning based genomic analysis methods enhanced our understanding for cancer research. However, the overfitting issue, arising from the limited number of patient samples, presents a challenge in improving the accuracy of genome analysis by deepening the neural network. Furthermore, it remains uncertain whether novel approaches such as the sparsely gated mixture of expert (MOE) and self-attention mechanisms can improve the accuracy of genomic analysis. We introduce a novel sparsely gated prognosis and classification analysis framework called Gene-MOE. This framework exploits the potential of the MOE layers and the proposed mixture of attention expert (MOAE) layers to enhance the analysis accuracy. Additionally, it addresses overfitting challenges by integrating pan-cancer information from 33 distinct cancer types through pre-training. According to the survival analysis results on 14 cancer types, Gene-MOE outperformed state-of-the-art models on 12 cancer types. Through detailed feature analysis, we found that the Gene-MOE model could learn rich feature representations of high-dimensional genes. According to the classification results, the total accuracy of the classification model for 33 cancer classifications reached 95.8%, representing the best performance compared to state-of-the-art models. These results indicate that Gene-MOE holds strong potential for use in cancer classification and survival analysis.

**Index Terms**—Survival analysis, Cancer classification, Genomic analysis, Mixture of expert, Self-attention.

## I. INTRODUCTION

Carcinogenic manifestations often result from mutations in one or more genes [1]. The Cancer Genome Atlas (TCGA) project represents a major advance in cancer genomics. The tens of thousands of pretreatment samples in TCGA, including over 30 cancer types and numerous measurements, including RNA sequencing (RNA-seq), DNA methylation, and copy-number variation, deepen our understanding of cancer-related genes and their clinical relevance [2]–[4]. To find more meaningful biological functions, researchers have developed methods such as prognosis prediction [5], [6], tumor subtypes [7], microsatellite instability (MSI) [8], immunological aspects [9], and certain pathways of interest [10].

Xiangyu Meng, Xue Li, Qing Yang, Huanhuan Dai, Lian Qiao, Hongzhen Ding, Long Hao and Xun Wang are with the Department of Computer Science and Technology, China University of Petroleum, Qingdao, Shandong, 266580, China (e-mail: x.meng@s.upc.edu.cn; Xueleecs@gmail.com; s21070069@s.upc.edu.cn; daihuanhuan0901@163.com; s21070055@s.upc.edu.cn; s22070050@s.upc.edu.cn; 1808010425@s.upc.edu.cn; wangsyun@upc.edu.cn) (*Corresponding author: Xun Wang*)

In the past two decades, a series of machine learning methods have been proposed for genomic analysis. Representative work includes gene survival analysis using the COX regression model [11], cancer classification and tumor biomarker identification using random forest [12], [13], cluster gene expression data using principal component analysis (PCA) [14], gene selection and cancer classification using support vector machine (SVM) [15], and gene expression pattern classification using the linear regression method [16]. Owing to their simplicity and user-friendliness, machine learning models have proved to be highly efficient in processing genomic analysis tasks, delivering commendable results across various functions, such as dimensional reduction and clustering visualization. However, the nonlinear biological characteristics inherent in high-dimensional genes cannot be effectively learned by the machine learning method, leading to precision loss in genomic analysis.

In recent years, deep learning methods have received widespread attention. With powerful fitting capabilities and more accurate prediction effects than traditional learning methods, deep learning methods can more effectively handle the potential correlation features of high-dimensional data. Many researchers have adopted deep learning methods for feature extraction and downstream prediction. Representative work includes the Cox-nnet model [17], DeepCC [18], DeepCues [19], PathCNN [20], and the cancer prognosis and classification method using a graph convolutional network (GCN) [21], [22]. Unlike machine learning methods, deep learning methods have greatly improved fitting performance and prediction accuracy, thus improving cancer diagnosis and prognosis. However, owing to the imbalance of samples between different cancer types and the few fitting samples for cancer types such as uterine carcinosarcoma (UCS), ocular melanoma (UVM), and large b-cell lymphoma (DLBC), deep learning methods must build two to four layers of a deep neural network (DNN) to prevent over-fitting problems, so the model cannot learn the deep correlations between high-dimensional genes. Recently, the pre-trained models have received widespread attention owing to their powerful feature learning capabilities. These models require training a network with billions of parameters to learn common features across various data samples and transferring weights to a specific task to capture the unique properties. Some notable models are transformer-based models [23], [24], which were first proposed in the natural language

processing field. They include dense models such as GPT-3 [25], Gopher [26], and the sparse model based on the mixture of expert (MOE) model [27], [28]. Moreover, many pre-training models have been introduced to solve biological problems and have achieved remarkable results, including BioBERT [29], DNABERT [30], and scBERT [31].

However, challenges persist in the application of pre-trained models to high-dimensional genetic data. First, the number of genes far exceeds the number of patient samples, and most genes contain no useful information for diagnosis and prognosis, exacerbating the risk of over-fitting during training. The TCGA dataset is estimated to contain over 50,000 genes, of which protein-coding genes make up approximately 21,000 [32], and most genes contain no useful information. Appropriate data preprocessing and augmentation methods must be designed to avoid meaningless information as much as possible. Second, a variety of genes often express together to cause cancer, and a strong correlation exists between different genes. Exploring such correlations from high-dimensional genetic features requires special consideration to design appropriate feature extraction methods tailored to genomic data.

In this work, we combined the principles of the MOE structure to create a pre-trained feature extraction model called Gene-MOE for high-dimensional RNA-seq gene expression data. This model combines the characteristics of MOE and uses 500 million parameters to fully learn the deep correlation features of high-dimensional genes and fit low-dimensional spatial features through the proposed unsupervised training strategy. We selected two common applications to use Gene-MOE for downstream prediction. According to the result, the Gene-MOE model achieved good performance for both types of tasks. Specifically, the main contributions were as follows:

- 1) We propose a sparsely gated RNA-seq analysis framework called Gene-MOE. Gene-MOE exploits the MOE layers to extract the features from high-dimensional RNA-seq genes. Furthermore, the self-attention mechanism is added to construct the MOAE model to further learn the deep semantic relationship inside the genetic features. Finally, we use a novel self-supervised pre-training strategy to make Gene-MOE learn the common features of 33 cancers and then transfer the pre-trained weight to the specific analysis including survival analysis and cancer classification;
- 2) According to the survival analysis results on 14 cancer types, the Gene-MOE achieved the best concordance index on 12 cancer types. Moreover, the classifier using pre-trained Gene-MOE achieved accurate classification of 33 cancer types, with a total accuracy of 95.8%;
- 3) According to the correlation analysis result, we found many cancer-related genes were strongly correlated with hidden nodes with high variance, which proves that Gene-MOE can effectively learn the gene expression of 33 types of cancer during the pre-training stage;
- 4) According to the visualization analysis, we found that the reconstructed genes coincided with the input genes during the pre-training phase, proving that Gene-MOE can perfectly learn the feature representation of high-dimensional genes.

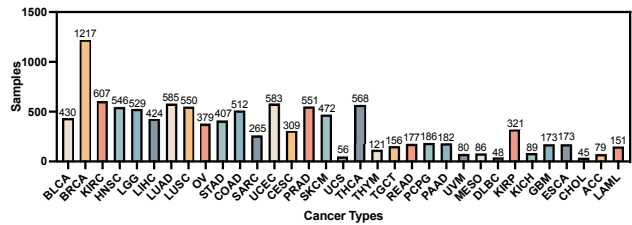


Fig. 1. Patient statistics of 33 cancer types after preprocessing.

The rest of this paper is organized as follows. Section II illustrates our method, including the dataset preparation, Gene-MOE framework illustration, and training strategy. Section III presents our experimental results for Gene-MOE. Finally, in Section IV, we provide our conclusion.

## II. METHODS

### A. Dataset Preparation

In this study, we primarily utilized the pan-cancer RNA-seq database from the TCGA dataset of the Pan-Cancer Atlas project, which consists of 33 cancer types. Furthermore, we downloaded the specific RNA-seq dataset for each TCGA cancer type. UCSC Xena already includes the preliminary processing for these 34 datasets, so we directly used the RNA-seq data after the FPKM-UQ normalization from UCSC Xena. In the initial dataset, each patient was associated with 60,484 genes, a majority of which exhibited null expression and had no relevance to cancer. Consequently, our first step involved filtering out these non-contributing genes. We first deleted the empty genes and selected overlapping genes among 34 datasets. Next, we filtered out genes with variances less than 0.4 and mean values less than 0.8 according to [22]. The reason is that genes that meet this low variance and low mean range were 0 in most patients and did not make any contribution to model training. Finally, before feeding the data into the network, we performed min-max normalization. After preparation, we selected 25,182 genes for each dataset. Figure 1 shows the patient number of these 33 cancer types.

### B. Framework Illustration

Figure 2 illustrates the framework of Gene-MOE, which comprises two stages: pre-training and fine-tuning. During the first stage, we construct the Gene-MOE model to learn low-dimensional feature encoding of high-dimensional pan-cancer genes. In this stage, we employ a self-supervised learning approach where the training labels are the input genes, aiming to acquire low-dimensional feature encoding of high-dimensional pan-cancer genes. The Gene-MOE model primarily consists of an encoder backbone network and a decoder network. Within the encoder network, we introduce an innovative MOE model based on sparse gating. This method involves multiple experts, enabling the encoder to learn rich feature representations of the genomic information. Moreover, we designed a MOAE model, which employs multiple attention mechanisms as distinct experts and uses a learnable sparse gating mechanism to merge attention features adaptively. In the second stage, the backbone

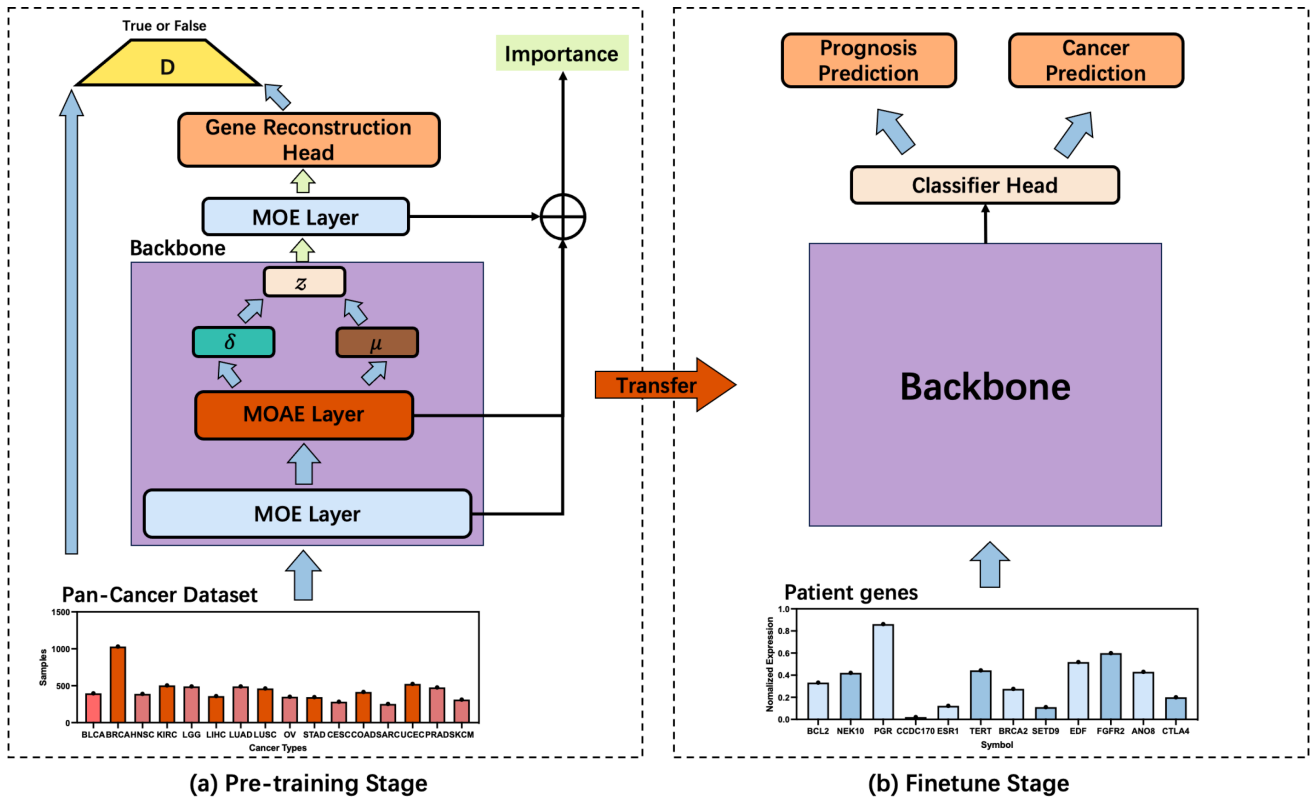


Fig. 2. Framework illustration of Gene-MOE. This model primarily consists of an encoder backbone network and a decoder network. (a) Pre-training stage. During this phase, Gene-MOE takes preprocessed pan-cancer genes as input to train the encoder-decoder network. (b) Fine-tuning stage. During this stage, Gene-MOE transfers the pre-trained backbone and connects to a classification head to achieve accurate downstream prediction tasks such as prognosis prediction, cancer classification, and specific pathways of interest.

of the Gene-MOE is transferred, and a new classification head is constructed to accomplish a fast, accurate downstream task after fine-tuning. This methodology enables us to fully leverage the Gene-MOE model in two stages, facilitating the learning of rich pan-cancer gene feature encoding and the achievement of excellent performance in multiple downstream tasks.

1) *Sparsely Gated MOE Layer*: Each patient has over 20,000 genes, among which intricate correlations exist. In previous work, it was common to build one or multiple fully connected networks (FCNs) to learn and extract key features related to genes. However, directly employing FCNs cannot effectively help the model learn these intricate correlations of high-dimensional gene input. The learned features would result in a substantial loss. In contrast to dense layers, the MOE module trains  $N$  experts, each of which independently learns and extracts features based on the characteristics of the input data. Compared with FCN, the MOE model can integrate diverse features from multiple expert models, enhancing the feature extraction capabilities of high-dimension genes and the overall model performance. Moreover, the training of each expert is independent, allowing for adjustments based on the characteristics of gene data, thus providing greater flexibility compared with fully connected layers. The MOE layer with

$N$  experts is denoted as

$$y = \sum_{i=1}^n G_i(x) \cdot D_i(x), \quad (1)$$

where  $D_i(x)$  is the expert network, which is an independent dense layer, and  $G_i(x)$  is the sparsity gating network. Throughout the training phase of the model,  $G_i(x)$  is employed to dynamically select the top  $K$  experts, expressed as

$$G(x) = \text{Softmax}(\text{TopK}(H(x), k)), \quad (2)$$

where  $\text{TopK}(H(x), k)$  denotes a discrete function that maps the input feature  $H(x)$  to a mask  $m \in \mathbb{R}^n$ . It is denoted as

$$\text{TopK}(H(x), k)_i = \begin{cases} H_i(x) & \text{if } H_i(x) \text{ in the top } K \text{ of } v. \\ -\infty & \text{otherwise.} \end{cases} \quad (3)$$

This equation generates  $m$ , in which the values in  $H(x)$  corresponding to elements outside the top  $K$  are set to  $-\infty$  so that when feeding  $m$  to softmax function, the corresponding elements are set to 0. Furthermore, to improve the load balance, we introduce the noise term to the input  $x$  and generate  $H(x)$ , denoted as

$$H_i(x) = (x \cdot W)_i + z \cdot \text{Softplus}((x \cdot W_{\text{noise}})_i), \quad (4)$$

where  $z \sim N(0, 1)$  is a random Gaussian noise,  $W$  is a trainable weight matrix that learns the sparsity gating feature, and  $W_{\text{noise}}$  is the weight that controls the noise increment.

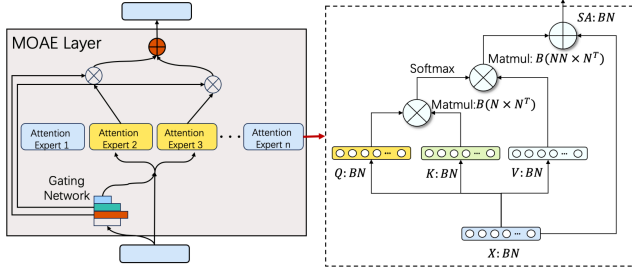


Fig. 3. Framework of Mixture of Attention Expert Layer (MOAE) layer

2) *Mixture of Attention Expert Layer*: Using self-attention mechanisms can effectively help the model learn deep semantics in high-dimensional features. However, owing to the excessively high dimensions of genetic features, the direct use of self-attention methods still leads to some loss of crucial information. Moreover, given the scarcity of samples, stacking multiple layers of self-attention modules may introduce overfitting issues. Therefore, we propose a mixture of attention expert (MOAE) model based on the MOE mechanism by constructing various attention experts and letting the model automatically choose the top  $K$  attention experts with better effects. Training this module effectively fuses features extracted by the top- $k$  self-attention experts, yielding richer semantic information. Unlike MOE, each expert in this module is a residual self-attention network, which is shown in Figure 3.

### C. Training Strategy

We constructed a self-supervised pre-training strategy to learn the common features of pan-cancer genes and improve the feature extraction performance of the backbone network.

1) *Data Augmentation by Gaussian Noise*: The Pan-cancer dataset had 10,000 patients after preprocessing. If we were to use 0.5 billion parameters, Gene-MOE might cause overfitting issues. Therefore, we built a data augmentation strategy by introducing Gaussian noise. For an input gene  $x$ , the augmented input  $\hat{x}$  is expressed as

$$\hat{x} = x + z, \quad (5)$$

where  $z \sim N(0, 0.2)$ . Moreover, the dropout strategy was introduced during the training.

2) *Joint Training Using a Generative Adversarial Network*: We used the training strategy of a generative adversarial network (GAN) to pre-train Gene-MOE. We constructed a discriminator called  $D$ , which is a dense layer network, and the Gene-MOE model is the generator. Then, Wasserstein loss was introduced to train  $G$  and  $D$  jointly. For  $G$  and  $D$ , the loss is denoted as

$$\mathcal{L}_{gan} = \mathbb{E}_{\hat{x} \sim P_{data}(\hat{x})} D(\hat{x}) - \mathbb{E}_{\hat{x} \sim P_{data}(\hat{x})} D(G(\hat{x})) - \lambda_{gp} \mathbb{E}_{\hat{x} \sim \mathcal{X}} \|\|\nabla_{\hat{x}} D(\hat{x})\|_2 - 1\|_2, \quad (6)$$

where  $\lambda_{gp}$  is the hyper-parameter of the gradient penalty, and  $\mathcal{X}$  is the sample space of  $x$  and  $\hat{x}$ . Training using Equation 6 can help Gene-MOE learn how to perform dimensional reduction and reconstruct the generated gene.

3) *Measuring the Distribution*: We further introduced the KL divergence to measure the similarity of the latent code  $z$  generated by  $\hat{x}$  and the standard Gaussian distribution. It can be denoted as

$$\mathcal{L}_{KL} = \sum_{i=0}^n (\mu(\hat{x})^2 + \sigma(\hat{x})^2 - \log(\sigma(\hat{x})^2) - 1), \quad (7)$$

where  $n$  represents the dim of  $z$ . Using this loss allows  $z$  to maintain a standard normal distribution, thus simplifying the training difficulty of Wasserstein loss.

4) *Measuring the Similarity of Genes*: We introduced L1 loss to further measure the similarity of each gene between samples reconstructed by Gene-MOE and the ground-truth samples. It is computed as

$$\mathcal{L}_{L1} = \|G(\hat{x}) - \hat{x}\|_1. \quad (8)$$

5) *Balancing Expert Utilization*: To allow each MOE layer to select each expert in a balanced manner, we introduced importance loss to each sparse gating layer of the MOE. The importance loss can be denoted as

$$\mathcal{L}_{importance} = \|Importance(f(\hat{x}))\|_2, \quad (9)$$

where  $f(\hat{x})$  denotes the input features of the gating layer, and  $Importance(f(\hat{x}))$  denotes

$$Importance(f(\hat{x})) = \sum_{i \in B} G(f(\hat{x})_i), \quad (10)$$

where  $B$  denotes the batch size of the input features, and  $G$  denotes the gating layer. To further improve the balanced loading, we also introduced the load balance loss  $\mathcal{L}_{load}$  in [27].

6) *Overall Pre-training Loss*: Combining these losses, we can express the overall loss of MOE as

$$\mathcal{L}_{total} = \mathcal{L}_{gan} + \lambda_{KL} \cdot \mathcal{L}_{KL} + \lambda_{L1} \cdot \mathcal{L}_{L1} + \lambda_{balance} \cdot (\mathcal{L}_{importance} + \mathcal{L}_{load}), \quad (11)$$

where  $\lambda_{KL}$ ,  $\mathcal{L}_{KL}$ ,  $\lambda_{L1}$ , and  $\lambda_{balance}$  are the hyper-parameters. Therefore, the pre-training stage aims to fit the optimal parameters  $\theta_G^*$  of MOE by solving

$$\theta_G^* = \arg \min_G \max_D \mathcal{L}_{total}. \quad (12)$$

### D. Experimental Settings

The Gene-MOE was implemented using the PyTorch framework. We trained and evaluated Gene-MOE using an NVIDIA Tesla V100 (32GB) GPU. During the pre-training stage, we initially trained the Gene-MOE model on the normalized pan-cancer dataset including 33 cancer types. We then randomly divided the pan-cancer data into train dataset and test dataset as a ratio of 4:1, where the train dataset was used for training and the test dataset was used for feature analysis. The Adam optimizer was used in the Gene-MOE training. During the pre-training stage, the learning rate of the optimizer was 0.0002, the total epochs were 200, and the batch size was 256. The hyper-parameters of the loss function were  $\lambda_{kl} = 10$ ,  $\lambda_{l1} = 20$ ,  $\lambda_{balance} = 10$ ,  $\lambda_{gp} = 10$ . For better convergence, we introduced a learning rate decay method that



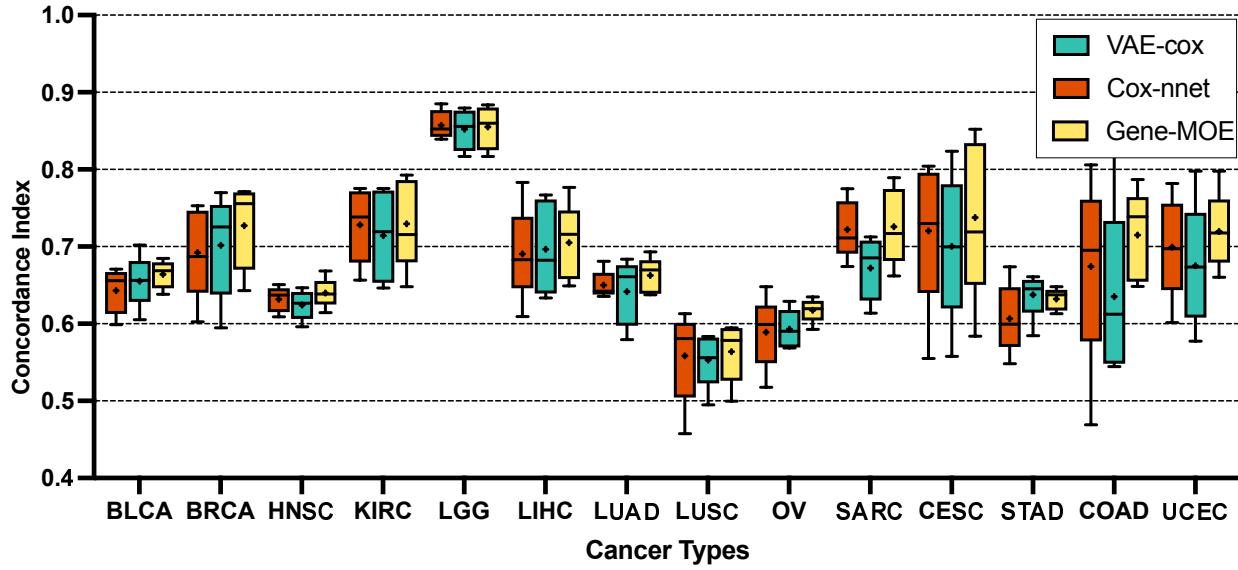


Fig. 5. Concordance Index Comparison of survival analysis on 14 cancer types. “+” of each box represents the mean Concordance Index.

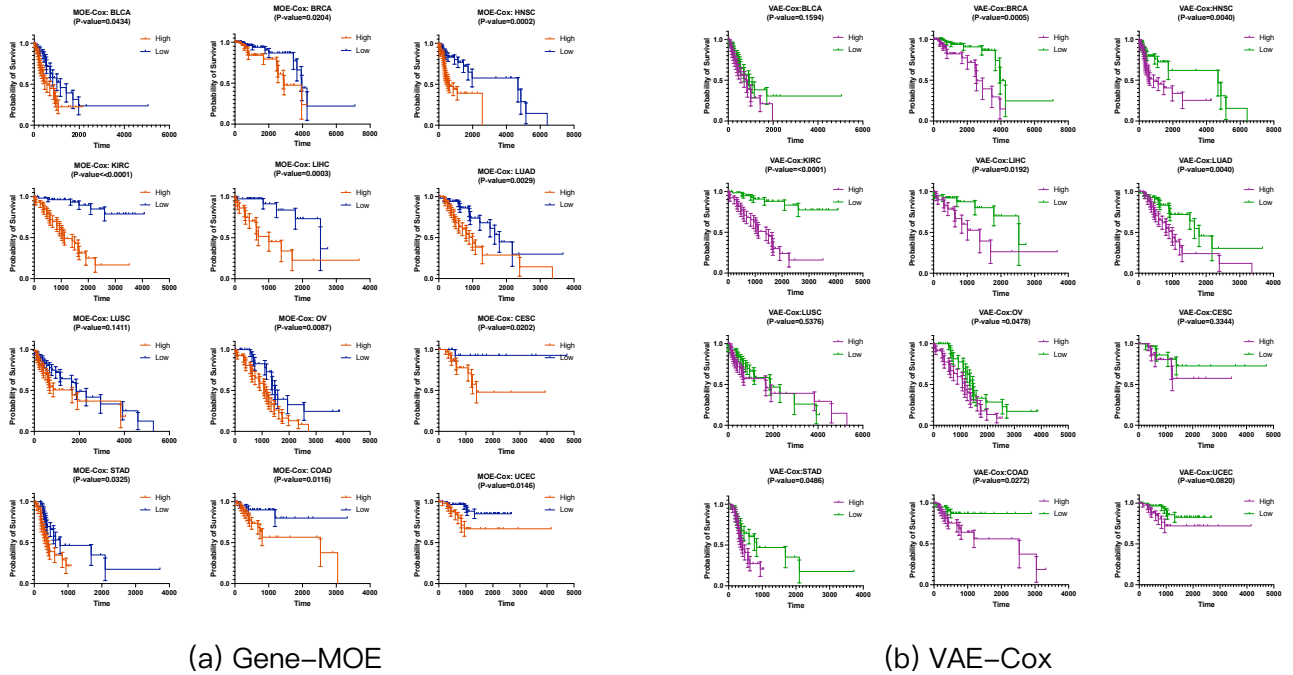


Fig. 6. Kaplan-Meier survival curves using MOE-Cox and VAE-cox on 12 cancer types. The Gene-MOE model shows a lower logP value on 10 cancer data sets. It shows that the Gene-MOE can predict hazard ratios that divide into high-risk groups and low-risk groups more significantly compared with VAE-cox on 10 cancer datasets.

*B. Performance on Cancer Type Classification*

We assessed the performance of Gene-MOE through a cancer classification task. Specifically, we designed a new classification head that takes the Gene-MOE’s backbone network as input, predicting probabilities for 33 distinct cancer types. Then Focal loss [35] was employed during the training process to mitigate the imbalance issue and enhance the model performance. Subsequently, we evaluated the precision, recall, and F1-score of the classification model employing Gene-MOE.

The performance results are depicted in Figure 4. As illustrated in this figure, our model demonstrated significant performance on 32 cancer types except rectum adenocarcinoma (READ), with a total accuracy of 95.8%.

To prove the novelty of proposed classifier, we selected several state-of-the-art classifiers for comparison, including classifier models based on machine learning methods such as random forest [36] and SVM [6], [36], as well as deep learning based classifier models like MLP [37] and CNN [38]. To ensure the fairness of the comparative experiments,

TABLE I  
COMPARISON OF CLASSIFICATION METRICS

	Accuracy	Precision	Recall	F1-Score
RandomForest	0.9010	0.8943	0.8338	0.8409
SVM	0.9498	0.9281	0.9114	0.9149
MLP	0.9250	0.8989	0.8756	0.8790
2D-Hybrid-CNN	0.9507	0.9300	0.9229	0.9232
Gene-MOE	<b>0.9580</b>	<b>0.9554</b>	<b>0.9374</b>	<b>0.9333</b>

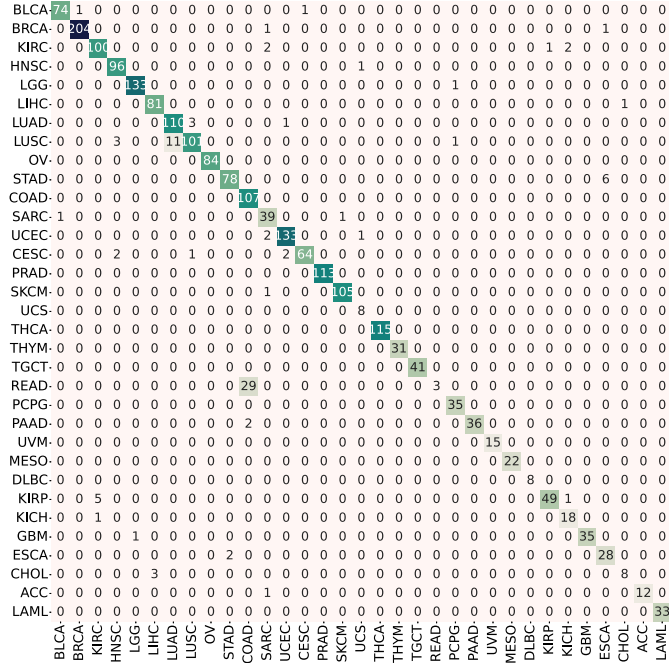


Fig. 7. Confusion matrix of test samples predicted by classification model using Gene-MOE with 33 cancer types.

we conducted five independent processes and calculated the average of the classification results to avoid the bias. Table I shows the classification result of these five models. According to table I, We found that the classification results of the Gene-MOE model on the test dataset was improved by 0.1-0.5 compared with the other four methods.

We further analyzed the classification performance by constructing a confusion matrix. Figure 7 illustrates the confusion matrix constructed for 33 types of cancer. Our model demonstrated accurate classification of all 33 cancer types with a notably low misclassification rate according to the confusion matrix. Moreover, we observed that our model misclassified 24 cases of READ as colon adenocarcinoma (COAD). This issue occurred because READ and COAD are genetically identical [39], and because COAD samples outnumbered READ samples, causing the model to misclassify some READ patients as COAD patients.

C. Feature Analysis of Gene-MOE

1) *Correlation Analysis:* We conducted a correlation analysis between the low-dimensional features extracted by the Gene-MOE model and the high-dimensional genes of patients. Specifically, we used 1,000 patient samples from the test

dataset to feed into the Gene-MOE model, and the model evaluated the low-dimensional features of each patient. We then selected the top 20 features with the highest variance as the leading features and calculated their Pearson correlations with the original patient genetic information. The results are shown in Figure 8(a), which presents a heat map illustrating the correlation between these leading features and the genes of 1,000 patients, which unequivocally indicates a significant correlation between the low-dimensional features predicted by the Gene-MOE model and the original input features. Based on Figure 8(a), we further refined our analysis by identifying genes with an average absolute correlation exceeding 0.4 with respect to the 20 leading features. Then, 29 strongly correlated genes were filtered, which is shown in Figure 8(b). According to the result in Figure 8(b), we observed that many genes with strong correlations to the leading features were cancer-related genes. For example, the TMPRSS4 gene is an emerging potential therapeutic target in cancer [40]. Moreover, tensin4 expression showed prognostic relevance in gastric cancer [41]. Furthermore, E2F1-initiated transcription of PRSS22 promoted breast cancer metastasis by cleaving ANXA1 and activating the FPR2/ERK signaling pathway [42]. In addition, down-regulation of FXD3 expression was observed in lung cancers [43]. Moreover, ST14 gene expression affected breast cancer [44]–[46]. In addition, RAB25 has been implicated in various cancers, with reports presenting it as both an oncogene and a tumor-suppressor gene [47], [48]. Long intergenic non-coding RNA 00324 promoted gastric cancer cell proliferation by binding with HuR and stabilizing FAM83B expression [49]. CBLC expression was found to be higher in breast cancer tissues and cells than in normal tissues and cells [50]. Furthermore, Serpin B5 was shown to be a CEA-interacting biomarker for colorectal cancer [51]. PKP3 interactions with the MAPK-JNK-ERK1/2-mTOR pathway regulated autophagy and invasion in ovarian cancer [52]. In addition, LAD1 expression was associated with the metastatic potential of colorectal cancer cells [53]. ELF3 was found to be a negative regulator of epithelial–mesenchymal transition in ovarian cancer cells [54]. Moreover, the expression patterns of CEACAM5 and CEACAM6 were observed in primary and metastatic cancers [55]. Grh12 determined the epithelial phenotype of breast cancers and promoted tumor progression [56]. KLF5 promoted breast cancer proliferation, migration, and invasion, in part by up-regulating the transcription of TNFAIP2 [57]. Finally, genetic predisposition to colon and rectal adenocarcinoma was found to be mediated by a super-enhancer polymorphism coactivating CD9 and PLEKHG6 [58].

2) *Visualization Analysis:* We further performed a visual analysis to measure the performance of Gene-MOE. We randomly selected 1,000 patients from the test set to perform this evaluation. The real gene expression of test patients was first fed into Gene-MOE to generate the reconstruction expression. Then, we used TSNE and UMAP to perform the visualization and evaluated the similarity of these two distributions. Figure 8(c) shows the visualization result using these two methods. According to Figure 8(c), the real gene distribution perfectly coincided with the reconstructed gene distribution, which proves that the Gene-MOE model can perform reconstruction

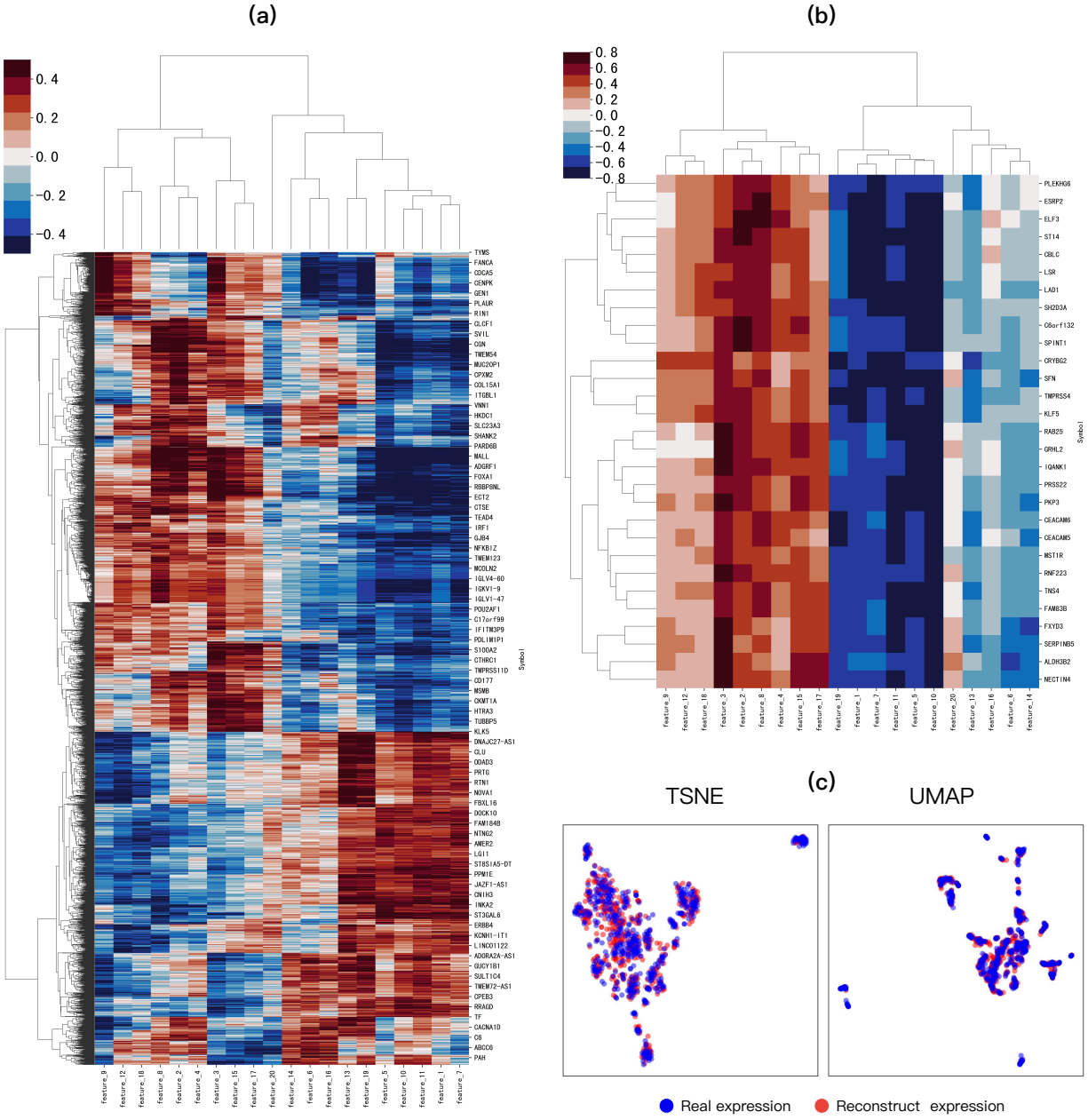


Fig. 8. Feature analysis of Gene-MOE. (a) Pearson correlation heat map between the leading feature and the patient genes. The features learned by Gene-MOE were strongly correlated with patient genes. (b) Pearson correlation heat map by selecting mean absolute coefficient greater than 0.5. (c) TSNE and UMAP results of real genes and Gene-MOE reconstructed genes. According to the results, the reconstructed genes maintained the same distribution as the real genes.

of the input genes more accurately based on the input real genes. Furthermore, Gene-MOE completed the reconstruction based on the low-dimensional feature obtained by the backbone model, which further reinforces that Gene-MOE can learn rich feature representation by the backbone network.

#### D. Ablation Studies

In this section, we extend our analysis by presenting ablation experiments conducted to evaluate the performance of the model proposed in this paper. Four distinct models were constructed for this purpose: 1) the baseline model comprising two FCN layers, 2) the model incorporating MOE by replacing

the FCN layers, 3) the Gene-MOE model, and 4) the pre-trained Gene-MOE model. Subsequently, survival analysis and cancer classification tasks were performed using these four models. The results of these tasks are presented in Tables II and III.

1) *Performance of MOE*: By comparing survival analysis result in Table II, we found the model with the MOE layer could achieve better Concordance results than baseline on 12 cancer types. Moreover, in Table III, the model with MOE showed better accuracy, and F1-score. These results indicate that using the MOE layer can increase the performance of genomic analysis, which proves our theory that using MOE can make a model learn rich features during the feature

TABLE II  
COMPARISON OF CONCORDANCE INDEX ON 14 CANCER TYPES USING FOUR DISTINCT MODELS

	BLCA	BRCA	HNSC	KIRC	LGG	LIHC	LUAD	LUSC	OV	SARC	CESC	STAD	COAD	UCEC
Baseline	0.643	0.692	0.632	0.728	0.857	0.691	0.649	0.558	0.590	0.722	0.720	0.607	0.674	0.699
MOE	0.670	0.711	<b>0.664</b>	0.729	0.848	0.700	0.663	0.596	0.616	0.733	0.720	0.641	0.705	0.712
MOAE	0.664	0.700	0.656	<b>0.730</b>	<b>0.850</b>	<b>0.713</b>	0.660	<b>0.599</b>	0.613	0.736	0.733	<b>0.728</b>	0.684	<b>0.719</b>
pre-train	<b>0.674</b>	<b>0.718</b>	0.649	<b>0.730</b>	<b>0.850</b>	0.708	<b>0.666</b>	0.590	<b>0.616</b>	<b>0.737</b>	<b>0.738</b>	0.630	<b>0.715</b>	0.716

TABLE III  
COMPARISON OF CLASSIFICATION METRICS USING FOUR DISTINCT MODELS

	Accuracy	Precision	Recall	F1-Score
Baseline	0.9304	0.9235	0.8721	0.8799
MOE	0.9417	0.9214	0.9063	0.9098
MOAE	<b>0.9584</b>	0.9469	0.9349	<b>0.9392</b>
pre-train	0.9580	<b>0.9554</b>	<b>0.9374</b>	0.9333

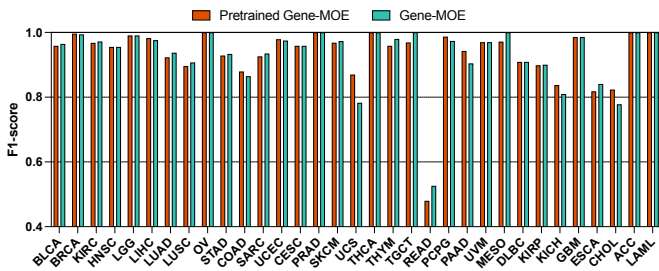


Fig. 9. Comparison of F1-score on 33 cancer types using pre-trained Gene-MOE and Gene-MOE.

extraction process.

2) *Performance of MOAE*: By comparing the Concordance Index for model with MOE and the Gene-MOE model in Table II, we observed that Gene-MOE outperformed the model with MOE on nine cancer types. Furthermore, in Table II, we found that Gene-MOE performed better in accuracy, precision, and F1-score. These findings prove that the MOAE model can further improve the accuracy of the model by improving the ability to learn deep semantic correlated features.

3) *Performance of Pre-training*: By comparing the performance of the Gene-MOE and pre-trained Gene-MOE models in Table II, we found that the pre-trained Gene-MOE model performed better in eight cancer types. At the same time, the Gene-MOE model demonstrated the same performance on KIRC and LGG datasets. These results reveal the effectiveness of pre-training, particularly in enhancing the performance of most survival analysis models. Further comparison of Gene-MOE and pre-trained Gene-MOE in Table III showed that that the pre-trained Gene-MOE model performed better in the precision and recall, but the accuracy and F1-score were lower than that of Gene-MOE. By further compare the F1-score of these two model in Figure 9, we found that the pre-trained model performed less effective on cancer types with few samples, such as the READ dataset. This discrepancy can be attributed to the fact that the pre-training stage primarily captures common cancer features, potentially missing certain characteristics for cancer types with small sample sizes. Con-

sequently, during the fine-tuning stage, the model tends to favor learning patterns from cancer types with larger sample sizes.

#### IV. CONCLUSION

In this work, we developed a sparsely gated model called Gene-MOE, which extensively leverages MOE layers to further deepen the ability to extract the deep correlation features of high-dimensional genes. Furthermore, we proposed a novel MOAE module to explore the deep semantic associations between high-dimensional genetic features. Finally, we designed novel pre-training strategies including data augmentation, self-supervised learning, and new loss functions to further improve the performance of Gene-MOE. The results show that Gene-MOE could achieve the best performance on cancer classification and survival analysis, indicating its strong potential for use in those applications. Currently, however, Gene-MOE has some limitations. During the pre-training stage, Gene-MOE focuses on cancer types with larger sample sizes, resulting in insufficient fitting of small sample datasets. Furthermore, the amount of existing data is insufficient, which leads to over-fitting issues in survival analysis and cancer classification tasks. In our future work, we aim to gather more genetic data for model training and to optimize the model training performance.

#### V. ACKNOWLEDGMENT

This work was supported by the National Key Research and Development Project of China under Grant 2021YFA1000103 and 2021YFA1000100, the National Natural Science Foundation of China under Grant 62372469, 61972416, 62272479 and 62202498, the Taishan Scholarship under Grant tsqn201812029, the Foundation of Science and Technology Development of Jinan under Grant 201907116, the Shandong Provincial Natural Science Foundation under Grant ZR2022LZH009 and ZR2021QF023, the Fundamental Research Funds for the Central Universities under Grant 21CX06018A, the Spanish project under Grant PID2019-106960GB-I00, the Juan de la Cierva under Grant IJC2018-038539-I.

#### REFERENCES

- [1] J. Liñares-Blanco *et al.*, “Machine learning analysis of tcga cancer data,” *PeerJ Computer Science*, vol. 7, p. e584, 2021.
- [2] Z. Zhang *et al.*, “A survey and evaluation of web-based tools/databases for variant analysis of tcga data,” *Briefings in bioinformatics*, vol. 20, no. 4, pp. 1524–1541, 2019.
- [3] Y. Li *et al.*, “Proteogenomic data and resources for pan-cancer analysis,” *Cancer Cell*, vol. 41, no. 8, pp. 1397–1406, 2023.

- [4] “Pan-cancer analysis of whole genomes,” *Nature*, vol. 578, no. 7793, pp. 82–93, 2020.
- [5] W. Zhu *et al.*, “The application of deep learning in cancer prognosis prediction,” *Cancers*, vol. 12, no. 3, p. 603, 2020.
- [6] K. Kourou *et al.*, “Machine learning applications in cancer prognosis and prediction,” *Computational and structural biotechnology journal*, vol. 13, pp. 8–17, 2015.
- [7] T. Sorlie *et al.*, “Repeated observation of breast tumor subtypes in independent gene expression data sets,” *Proceedings of the national academy of sciences*, vol. 100, no. 14, pp. 8418–8423, 2003.
- [8] R. J. Hause *et al.*, “Classification and characterization of microsatellite instability across 18 cancer types,” *Nature medicine*, vol. 22, no. 11, pp. 1342–1350, 2016.
- [9] J. Sanchez and J. Holmgren, “Cholera toxin structure, gene regulation and pathophysiological and immunological aspects,” *Cellular and molecular life sciences*, vol. 65, pp. 1347–1360, 2008.
- [10] K. Wang *et al.*, “Analysing biological pathways in genome-wide association studies,” *Nature Reviews Genetics*, vol. 11, no. 12, pp. 843–854, 2010.
- [11] D. Y. Lin and L.-J. Wei, “The robust inference for the cox proportional hazards model,” *Journal of the American statistical Association*, vol. 84, no. 408, pp. 1074–1078, 1989.
- [12] D. Capper *et al.*, “Dna methylation-based classification of central nervous system tumours,” *Nature*, vol. 555, no. 7697, pp. 469–474, 2018.
- [13] R. Díaz-Uriarte and S. Alvarez de Andrés, “Gene selection and classification of microarray data using random forest,” *BMC bioinformatics*, vol. 7, pp. 1–13, 2006.
- [14] K. Y. Yeung and W. L. Ruzzo, “Principal component analysis for clustering gene expression data,” *Bioinformatics*, vol. 17, no. 9, pp. 763–774, 2001.
- [15] K.-B. Duan *et al.*, “Multiple svm-rfe for gene selection in cancer classification with expression data,” *IEEE transactions on nanobioscience*, vol. 4, no. 3, pp. 228–234, 2005.
- [16] S. Liu *et al.*, “Prediction of gene expression patterns with generalized linear regression model,” *Frontiers in Genetics*, vol. 10, p. 120, 2019.
- [17] T. Ching *et al.*, “Cox-nnet: an artificial neural network method for prognosis prediction of high-throughput omics data,” *PLoS computational biology*, vol. 14, no. 4, p. e1006076, 2018.
- [18] F. Gao *et al.*, “Deepcc: a novel deep learning-based framework for cancer molecular subtype classification,” *Oncogenesis*, vol. 8, no. 9, p. 44, 2019.
- [19] Z. Zeng *et al.*, “Deep learning for cancer type classification and driver gene identification,” *BMC bioinformatics*, vol. 22, no. 4, pp. 1–13, 2021.
- [20] J. H. Oh *et al.*, “Pathcnn: interpretable convolutional neural networks for survival prediction and pathway analysis applied to glioblastoma,” *Bioinformatics*, vol. 37, no. Supplement\_1, pp. i443–i450, 2021.
- [21] R. Ramirez *et al.*, “Classification of cancer types using graph convolutional neural networks,” *Frontiers in physics*, vol. 8, p. 203, 2020.
- [22] —, “Prediction and interpretation of cancer survival using graph convolution neural networks,” *Methods*, vol. 192, pp. 120–130, 2021.
- [23] X. Li *et al.*, “Marppi: boosting prediction of protein–protein interactions with multi-scale architecture residual network,” *Briefings in Bioinformatics*, vol. 24, no. 1, p. bbac524, 2023.
- [24] X. Wang *et al.*, “Transfusionnet: Semantic and spatial features fusion framework for liver tumor and vessel segmentation under jetsontx2,” *IEEE Journal of Biomedical and Health Informatics*, vol. 27, no. 3, pp. 1173–1184, 2022.
- [25] T. Brown *et al.*, “Language models are few-shot learners,” *Advances in neural information processing systems*, vol. 33, pp. 1877–1901, 2020.
- [26] J. W. Rae *et al.*, “Scaling language models: Methods, analysis & insights from training gopher,” *arXiv preprint arXiv:2112.11446*, 2021.
- [27] N. Shazeer *et al.*, “Outrageously large neural networks: The sparsely-gated mixture-of-experts layer,” in *5th International Conference on Learning Representations, ICLR 2017, Toulon, France, April 24–26, 2017, Conference Track Proceedings*. OpenReview.net, 2017.
- [28] D. Lepikhin *et al.*, “Gshard: Scaling giant models with conditional computation and automatic sharding,” in *9th International Conference on Learning Representations, ICLR 2021, Virtual Event, Austria, May 3–7, 2021*. OpenReview.net, 2021.
- [29] J. Lee *et al.*, “Biobert: a pre-trained biomedical language representation model for biomedical text mining,” *Bioinformatics*, vol. 36, no. 4, pp. 1234–1240, 2020.
- [30] Y. Ji *et al.*, “Dnabert: pre-trained bidirectional encoder representations from transformers model for dna-language in genome,” *Bioinformatics*, vol. 37, no. 15, pp. 2112–2120, 2021.
- [31] F. Yang *et al.*, “scbert as a large-scale pretrained deep language model for cell type annotation of single-cell rna-seq data,” *Nature Machine Intelligence*, vol. 4, no. 10, pp. 852–866, 2022.
- [32] M. Pertea *et al.*, “Thousands of large-scale rna sequencing experiments yield a comprehensive new human gene list and reveal extensive transcriptional noise,” *BioRxiv*, p. 332825, 2018.
- [33] S. Kim *et al.*, “Improved survival analysis by learning shared genomic information from pan-cancer data,” *Bioinformatics*, vol. 36, no. Supplement\_1, pp. i389–i398, 2020.
- [34] H. Steck *et al.*, “On ranking in survival analysis: Bounds on the concordance index,” *Advances in neural information processing systems*, vol. 20, 2007.
- [35] T.-Y. Lin *et al.*, “Focal loss for dense object detection,” in *Proceedings of the IEEE international conference on computer vision*, 2017, pp. 2980–2988.
- [36] A. Statnikov *et al.*, “A comprehensive comparison of random forests and support vector machines for microarray-based cancer classification,” *BMC bioinformatics*, vol. 9, no. 1, pp. 1–10, 2008.
- [37] T. Ahn *et al.*, “Deep learning-based identification of cancer or normal tissue using gene expression data,” in *2018 IEEE international conference on bioinformatics and biomedicine (BIBM)*. IEEE, 2018, pp. 1748–1752.
- [38] M. Mostavi *et al.*, “Convolutional neural network models for cancer type prediction based on gene expression,” *BMC medical genomics*, vol. 13, pp. 1–13, 2020.
- [39] C. G. A. Network *et al.*, “Comprehensive molecular characterization of human colon and rectal cancer,” *Nature*, vol. 487, no. 7407, p. 330, 2012.
- [40] A. De Aberasturi and A. Calvo, “Tmprss4: an emerging potential therapeutic target in cancer,” *British journal of cancer*, vol. 112, no. 1, pp. 4–8, 2015.
- [41] K. Sakashita *et al.*, “Prognostic relevance of tensin4 expression in human gastric cancer,” *Annals of Surgical Oncology*, vol. 15, pp. 2606–2613, 2008.
- [42] L. Song *et al.*, “E2f1-initiated transcription of prss22 promotes breast cancer metastasis by cleaving anxa1 and activating fpr2/erk signaling pathway,” *Cell Death & Disease*, vol. 13, no. 11, p. 982, 2022.
- [43] K. Okudela *et al.*, “Down-regulation of fxyd3 expression in human lung cancers: its mechanism and potential role in carcinogenesis,” *The American journal of pathology*, vol. 175, no. 6, pp. 2646–2656, 2009.
- [44] J. M. Kauppinen *et al.*, “St14 gene variant and decreased matriptase protein expression predict poor breast cancer survival,” *Cancer epidemiology, biomarkers & prevention*, vol. 19, no. 9, pp. 2133–2142, 2010.
- [45] Y. Wang *et al.*, “St14 (suppression of tumorigenicity 14) gene is a target for mir-27b, and the inhibitory effect of st14 on cell growth is independent of mir-27b regulation,” *Journal of Biological Chemistry*, vol. 284, no. 34, pp. 23 094–23 106, 2009.
- [46] Y.-H. Dai *et al.*, “Gene-associated methylation status of st14 as a predictor of survival and hormone receptor positivity in breast cancer,” *BMC cancer*, vol. 21, no. 1, pp. 1–14, 2021.
- [47] S. Mitra *et al.*, “Rab25 in cancer: a brief update,” *Biochemical Society Transactions*, vol. 40, no. 6, pp. 1404–1408, 2012.
- [48] S. Wang *et al.*, “Rab25 gtpase: Functional roles in cancer,” *Oncotarget*, vol. 8, no. 38, p. 64591, 2017.
- [49] Z. Zou *et al.*, “Long intergenic non-coding rna 00324 promotes gastric cancer cell proliferation via binding with hur and stabilizing fam83b expression,” *Cell death & disease*, vol. 9, no. 7, p. 717, 2018.
- [50] W. Li *et al.*, “Cblc inhibits the proliferation and metastasis of breast cancer cells via ubiquitination and degradation of ctnn,” *Journal of Receptors and Signal Transduction*, vol. 42, no. 6, pp. 588–598, 2022.
- [51] J. Y. Baek *et al.*, “Serpin b5 is a cea-interacting biomarker for colorectal cancer,” *International journal of cancer*, vol. 134, no. 7, pp. 1595–1604, 2014.
- [52] V. Lim *et al.*, “Pkp3 interactions with mapk-jnk-erk1/2-mtor pathway regulates autophagy and invasion in ovarian cancer,” *Biochemical and biophysical research communications*, vol. 508, no. 2, pp. 646–653, 2019.
- [53] B. Moon *et al.*, “Lad1 expression is associated with the metastatic potential of colorectal cancer cells,” *BMC cancer*, vol. 20, pp. 1–12, 2020.
- [54] T.-L. Yeung *et al.*, “Elf3 is a negative regulator of epithelial-mesenchymal transition in ovarian cancer cells,” *Oncotarget*, vol. 8, no. 10, p. 16951, 2017.
- [55] R. D. Blumenthal *et al.*, “Expression patterns of ceacam5 and ceacam6 in primary and metastatic cancers,” *BMC cancer*, vol. 7, pp. 1–15, 2007.
- [56] X. Xiang *et al.*, “Grhl2 determines the epithelial phenotype of breast cancers and promotes tumor progression,” *PloS one*, vol. 7, no. 12, p. e50781, 2012.

- [57] L. Jia *et al.*, “Klf5 promotes breast cancer proliferation, migration and invasion in part by upregulating the transcription of tnfai2,” *Oncogene*, vol. 35, no. 16, pp. 2040–2051, 2016.
- [58] J. Ke *et al.*, “Genetic predisposition to colon and rectal adenocarcinoma is mediated by a super-enhancer polymorphism coactivating cd9 and plekhg6,” *Cancer Epidemiology, Biomarkers & Prevention*, vol. 29, no. 4, pp. 850–859, 2020.